

IN VITRO ANALYSIS OF SURFACE MODIFIED
STAIN-ETCHED POROUS SILICON
MICROPARTICLES

by

Nancy Wareing

Submitted in partial fulfillment of the
requirements for Departmental Honors in
the Department of Biology
Texas Christian University
Fort Worth, Texas

May 5, 2014

IN VITRO ANALYSIS OF SURFACE MODIFIED
STAIN-ETCHED POROUS SILICON
MICROPARTICLES

Project Approved:

Supervising Professor: Giridhar Akkaraju, Ph.D.

Department of Biology

Jeffery Coffey, Ph.D.

Department of Chemistry

Michael Chumley, Ph.D.

Department of Biology

ABSTRACT

There is a growing need for efficient, biocompatible delivery methods to transport therapeutic genetic material and drugs to specific sites in the body. For the former goal, the successful delivery of genetic material (e.g., DNA, RNA, and oligonucleotides) to cells is a critical step for gene therapy. Nano-scale porous silicon (pSi) materials offer advantages over traditional viral transfection vectors as a consequence of their broadly tunable range of porosities, established surface modification protocols, and high surface area-to-volume ratio. While anodization of silicon wafers remains the most common preparative method for pSi formation, low cost/high throughput production makes stain-etching of metallurgical-grade silicon powder a practical alternative. Surface oxidation of stain-etch derived pSi provides ample sites for further functionalization and electrostatic coupling, as well as high bioavailability as demonstrated by *in vitro* and *in vivo* studies of similar materials. In this work we modified nanostructured porous silicon microparticles (SiMPs) using an aminosilanization route and developed an efficient protocol for fluorescent labeling with a fluorescein derivative. This material was then subjected to a novel dispersion method yielding the optimum concentration for *in vitro* studies. Upon addition to human embryonic kidney (HEK293) cells, we observed no cytotoxicity and a high affinity interaction between the modified SiMPs and the cell surface. Immunofluorescence staining of the cytoskeleton of HEK293 cells and confocal imaging revealed adsorption of fluorescently labeled SiMPs onto the cell membrane. By demonstrating the biocompatibility and high-affinity membrane interaction of surface oxidized, metal-assisted stain-etched mesoporous silicon microparticles with HEK293 cells, we present the possibility of using such material for transfection and gene delivery.

ACKNOWLEDGEMENTS

We acknowledge the TCU IS initiative (Giridhar Akkaraju, Jeffery L. Coffey), the TCU Department of Biology (Nancy Wareing, Giridhar Akkaraju), the Robert A. Welch Foundation (Jeffery L. Coffey), and the NIH (Jeffery L. Coffey) for their financial support of this research.

TABLE OF CONTENTS

INTRODUCTION	1
Gene therapy	1
Porous silicon nanotechnology	1
MATERIALS AND METHODS	4
Chemicals	4
Cell culture.....	4
Preparation and characterization of silicon microparticles.....	5
Trypan Blue exclusion assay	5
Aminosilanization of silicon microparticles	6
Coupling of fluorescein isothiocyanate to silicon microparticles.....	6
Confocal fluorescence microscopy.....	6
Dispersion via ultra-sonication	6
Treatment of HEK293 cells with dispersed silicon microparticles	7
Immunofluorescence.....	7
Plasmid	8
DNA binding.....	8
Surfactant-free transfection of cultured cells.....	9
Surfactant-supplemented transfection of cultured cells	10
RESULTS	11
Stain-etch preparation of silicon microparticles	11
Biocompatibility of silicon microparticles	11
Aminosilanization	13

FITC-coupling and imaging	14
Dispersion	16
Cellular interaction with fluorescently labeled silicon microparticles	17
DNA binding	19
Transfection with plasmid DNA	20
DISCUSSION	22
REFERENCES	24

LIST OF FIGURES

FIGURE 1	12
FIGURE 2	13
FIGURE 3	13
FIGURE 4	14
FIGURE 5	15
FIGURE 6	17
FIGURE 7	18
FIGURE 8	18
FIGURE 9	19
FIGURE 10	21

INTRODUCTION

Gene therapy

Gene therapy is a growing field of research, which centers on the potential of using nucleic acids (e.g. DNA, RNA, oligonucleotides) to treat diseases with specific tropisms. The nucleic acid used for gene therapy usually encodes either a therapeutic protein or inhibits the expression of a detrimental gene¹. A novel advantage of gene therapy over more traditional treatments is the self-propagation of the therapeutic gene in the target cell line. The successful delivery of genetic material to cells is a critical step for *in vivo* gene therapy^{2,3}. When intravenously injected, naked plasmid DNA is rapidly cleared from systemic circulation and degraded by the mononuclear phagocyte system³. Historically viral vectors have been used to introduce therapeutic genes into cells; however viral-mediated techniques have a number of risks including pathogenesis, immunogenesis, and insertional mutagenesis^{1,2}. As such, there is a growing need for efficient, biocompatible, non-viral delivery methods to transport therapeutic genetic material and drugs to specific sites in the body. The high bioactivity of gene products makes transgene expression in non-target sites a potential source of side effects. Therefore, ideal vectors will have the ability to target delivery and expression of the therapeutic gene to specific cells, tissues, or organs³. An emerging area of study is the use of inorganic nanomaterial for targeted gene delivery.

Porous silicon nanotechnology

Nanotechnology is a growing field of biomedical research and therapeutics, which is already beginning to transform clinical diagnostics and treatment⁴. Nano-scale diagnostic methods are already in use, including paramagnetic iron oxide nanoparticles

for magnetic resonance imaging⁴. As of 2012, over two-dozen nanoparticle-based materials have been approved for a wide variety of clinical uses⁵. Furthermore, a number of promising treatment applications of nanotechnology are in clinical trials and even more are in the preclinical phases of development, many of which focus on drug targeting and delivery⁴.

Nanotechnology refers to the application of nano-scale materials for use in technology and biomedicine. A subcategory of nanotechnology is nanomedicine, which specifically focuses on the use of such materials for medical science, including therapeutics and imaging⁶. Although there seems to be no consistent size classification standards for nanomaterials, nano-scale materials tend to be or possess individual features, such as pores, in the size range of 1-100 nm. At the nano-scale, the properties of elements change dramatically; however the size at which novel properties appear is material-dependent^{5,6,7}. These advantageous properties include, but are not limited to, increased surface area-to-volume ratios, and enhanced ability to cross biological barriers^{8,9}. The manufacturing of nanomaterials also makes them logistically preferable to larger molecular drugs because of their smaller physical size⁵. In addition, a single nanostructure can be used for diagnostics, treatment, and targeting⁵. Inorganic materials and polymers show promise for numerous biomedical applications⁵.

Nano-scale porous silicon (pSi) materials offer advantages over traditional viral gene delivery vectors as a consequence of their broadly tunable range of porosities, established surface modification protocols, high surface area-to-volume ratio, and ability to degrade in aqueous solution^{7,10}. pSi is an attractive material for gene therapy because of the ability to add a high amount of DNA to a large modified surface area. High levels

of pSi-bound DNA may alleviate issues such as the low efficiency of transfection previously reported with other vectors like polyethylene glycolated liposomes³. An additional advantage of using porous silicon for *in vivo* application is the degradation of pSi materials to silicic acid, Si(OH)₄, the most prominent form of silicon in the human body which can be quickly excreted in the urine^{11,12}.

The three most predominant pSi nanostructures currently being investigated for biotechnical applications include nanowires, nanotubes, and nanoparticles⁷. Silicon nanowires can be manufactured through a number of processes, some of which can produce nanowires with aspect ratios, the relation width and height, greater than 200:1¹³. Nanotubes have been synthesized via silane deposition on nanowire arrays of other materials such as zinc oxide¹⁴. pSi nanoparticles are commonly produced via anodization of silicon wafers followed by a milling or grinding step¹⁵. However another process referred to as “stain-etching” can produce micro- and nano-scale pSi materials with greater ease¹⁵. A single nanoparticle commonly has an aspect ratio of approximately 1, while nanowires and nanotubes have significantly higher aspect ratios¹⁶. Delicate control over pore sizes is possible and larger pore sizes have been shown to increase the rate of degradation of surface-oxidized pSi nanoparticles¹⁷.

A related material to elemental silicon is silica, or SiO₂. *In vitro* and *in vivo* studies have investigated both silica nanoparticles and nanotubes¹⁶. Silica nanoparticles demonstrated lower toxic effects *in vivo* than nanotubes¹⁶. Non-toxic, organically modified silica nanoparticles can facilitate successful *in vivo* transfection and genetic modulation of mouse neural cells². While such silica nanomaterials have shown promise as transfection vectors, recent work demonstrated that silica nanoparticles were toxic to

hepatocytes and resulted in liver damage *in vivo*¹⁸. The ease of the stain-etch porofication of elemental silicon offers distinct and novel advantages for the applications of these micro-scale materials possessing nano-scale properties. We seek to investigate the possibility of using stain-etched, surface-modified pSi microparticles for gene delivery.

MATERIALS AND METHODS

Chemicals

3-aminopropyl triethoxysilane (APTES), Dulbecco's Modified Eagle's Medium, Trypan Blue Solution (0.4%), penicillin-streptomycin solution (10,000 units penicillin and 10 mg streptomycin/mL in 0.9% NaCl), and L-glutamine (200 mM) were obtained from Sigma Aldrich Co. LLC (St. Louis, MO, USA). Fluorescein isothiocyanate isomer 1 (FITC) was obtained from Gelest, Inc. (Tullytown, PA, USA). Triple 0.1 um filtered fetal bovine serum (FBS) was obtained from Atlanta Biologicals, Inc. (Lawrenceville, GA, USA). Ampicillin was obtained from Bio-Rad Laboratories, Inc. (Hercules, CA, USA). Dual-Luciferase Reporter Assay System was obtained from Promega Corporation (Madison, WI, USA). 4-(2-Hydroxyethyl)-1-Piperazineethanesulfonic Acid (HEPES) was purchased from Fisher Scientific. Antibodies were purchased from Santa Cruz Biotechnology, Inc. (Dallas, Texas, USA). Lyovec™ was obtained from InvivoGen (San Diego, California, USA).

Cell culture

Cells were maintained in Dulbecco's Modified Eagle's Medium (DMEM) supplemented with 10% (vol/vol) FBS, penicillin [89.3 units/mL], streptomycin [0.089 mg/mL], and glutamine [1.96 mM]. Human embryonic kidney (HEK293) cells are a commonly used immortalized cell line. The HeLa cell line (ATCC® CCL-2™) is an

immortalized cervical cancer cell line. Cells were maintained at 37°C with 5% CO₂ in air, in a humidified incubator.

Preparation and characterization of silicon microparticles

Porous silicon microparticles (SiMPs) were obtained from Intrinsic Materials Ltd (Malvern, UK). Preparation and characterization was conducted by a previously reported technique¹⁵. Metallurgical-grade silicon powder was subjected to metal-assisted stain-etching using hydrofluoric acid and ferric ion to produce so-called stain etched SiMPs¹⁵. The material was then subjected to surface oxidation by static annealing in air at 800°C for 1 h¹⁵. The size distribution is as follows, where “D” is diameter: D₁₀=0.7 μm, D₅₀=2.2 μm, D₉₀=8.9 μm¹⁵. The corresponding mean surface area of the material as measured by Brunauer-Emmett-Teller (BET) isotherms was 356 m²/g with an associated pore volume of 0.292 ml/g and average pore diameter of 3.5 nm-4.7 nm¹⁵.

Trypan Blue exclusion assay

HEK293 cells were seeded at a density of 1x10⁴ cells/mL in a 24 well tray and allowed to incubate at 37°C with 5% CO₂ in air, in a humidified incubator for 24 h prior to treatment. SiMPs (30, 3.0, and 0.3 mg) were weighed out using a standard top-loading balance. Indicated amounts were then soaked in 1 mL 99.9% ethanol at room temperature in a sterile hood until ethanol evaporated completely. The given amounts of SiMPs were added to 6 mL DMEM complete medium. Aliquots (1 mL) of SiMPs in medium were added to wells of a 24 well tray. Cells were allowed to incubate at 37°C with 5% CO₂ in air, in a humidified incubator for 24 h prior to assay. After the medium was removed, cells were washed with PBS (1X) and trypsinized with 0.25 mL trypsin. Volumes were brought to 1 mL with medium and triturated cell suspensions were added to sterile

Eppendorf tubes. Suspensions were centrifuged at 10,000 rpm for 3 min. The supernatant was removed and 0.25 mL serum-free medium followed by 0.05 mL Trypan Blue Solution (0.4%) was added to the tubes. The solution was triturated 3 times to re-suspend the pellet. Suspensions were rocked for 5 min at room temperature. Suspensions were triturated 20 times. Cells were visualized and counted using a Bright Line hemocytometer.

Aminosilanization of silicon microparticles

SiMPs were added to a 1% (vol/vol) solution of APTES in acetone and allowed to sit covered for 4 h. SiMPs were washed with DI water.

Coupling of fluorescein isothiocyanate to silicon microparticles

APTES-functionalized SiMPs were prepared according to indicated procedure. SiMPs were then added to a 5 mM solution of fluorescein isothiocyanate (FITC) [$\lambda_{\text{ex}}=490$ nm, $\lambda_{\text{em}}=525$ nm] in DI water. SiMPs in FITC solution were allowed to incubate covered at 3°C over night. FITC solution was removed and SiMPs were washed 10 times with DI water.

Confocal fluorescence microscopy

Confocal fluorescence microscopy was carried out on Zeiss LSM710 laser-scanning confocal microscope.

Dispersion via ultra-sonication

Two separate dispersion protocols were investigated. In Protocol I, FITC-conjugated SiMPs were subjected to ultra-sonication in DMEM for 10 s at 5-6 W with a probe sonicator. In Protocol II, FITC-conjugated SiMPs were subjected to ultra-sonication in DMEM for 3 min at 5-6 W on ice. A Sonics Vibra-cell 130PB ultrasonic

processor at a frequency of 20kHz (Sonics & Materials Inc., Newtown, CT, USA) was used for all ultra-sonication procedures.

Treatment of HEK293 cells with dispersed silicon microparticles

HEK293 cells were seeded at a density of 4.0×10^4 cells/mL on sterile glass cover slips in 35 mm dishes. Cells were allowed to incubate at 37°C with 5% CO₂ in air, in a humidified incubator for 24 h prior to treatment. SiMPs were soaked in 1 mL 99.9% ethanol at room temperature in a sterile hood until ethanol evaporated completely. SiMPs were then weighed out on a standard top-loading balance and suspended in DMEM complete medium at a concentration of 4 µg/µL. Total volume was divided equally into sterile Eppendorf tubes. SiMP suspensions were then subjected to ultra-sonication using dispersion Protocol I. Suspensions were then centrifuged at 3,000 rpm for 1 min. Medium was removed from the cells. The supernatant of the suspension was then added to the cover slips. The cells were incubated at 37°C for 30 min. Total volume of medium in the wells was brought to 1 mL and cells were incubated at 37°C for 48 h prior to visualization.

Immunofluorescence

Cells were washed with phosphate buffered saline (PBS) [137 mM NaCl, 2.7 mM KCl, 4.3 mM Na₂PO₄·H₂O, 1.4 mM KH₂PO₄]. A volume of 4% paraformaldehyde sufficient to cover the cover slips was added to the cells. Cells were incubated at room temperature for 30 min then the paraformaldehyde was removed. Cells were incubated at room temperature for 15 min in PBS/0.2% Triton X-100. After PBS/0.2% Triton X-100 was removed, a 10% solution of goat serum in PBS was added to the cells and incubated for 1 h at room temperature. After the solution was removed, 1 mL of anti-β-actin mouse

monoclonal IgG in PBS [1:500 vol/vol] was added to each well. Wells were sealed with parafilm and allowed to incubate at 4°C over night on a rocker. After a wash step with PBS/0.5% Tween-20, 1 mL of Alexa Fluor 546 goat anti-mouse IgG (H+L) [1:1000] was added to the wells. Cells were incubated at room temperature for 1 h. The antibody solution was removed and cells were washed with PBS/0.5% Tween-20. Cover slips were mounted on glass slides with Fluoromount Aqueous Mounting Medium and cells were observed via confocal fluorescence microscopy.

Plasmid

Preparation was conducted using proper aseptic technique. 30 μ L AMP-LB [1 μ L/mL] in 30 mL LB was added to a 50 mL centrifuge tube and incubated overnight with bacteria transformed with a plasmid with the cytomegalovirus immediate-early gene promoter driving expression of the β -galactosidase gene (CMV IEp-LacZ). The CMV IEp-LacZ plasmid is a commonly used reporter plasmid. Bacterial suspensions were shaken overnight at 37°C at 200 rpm. The plasmid was then purified using the Genesee Scientific Zyppy Plasmid Midiprep protocol.

DNA binding

A 25 mM solution of HEPES (pH 7.4), an organic chemical buffering agent, was prepared. APTES-functionalized SiMPs were then added to the HEPES solution to a final concentration of 116 mg/mL. Suspension was subjected to ultra-sonication via Protocol II. Seven solutions were prepared in sterile Eppendorf tubes: (1) 106 μ L/mL CMV IEp-LacZ in HEPES; (2) 106 μ L/mL CMV IEp-LacZ and 10.1 μ L/mL SiMPs in HEPES; (3) 106 μ L/mL CMV IEp-LacZ and 106 μ L/mL SiMPs in HEPES; and (4) 106 μ L/mL CMV IEp-LacZ and 10.6 μ g/ μ L SiMPs in HEPES; (5) 106 μ L/mL CMV IEp-LacZ, 10.1

$\mu\text{L}/\text{mL}$ SiMPs, and 1.5% (vol/vol) Triton X-100 in HEPES; (6) 106 $\mu\text{L}/\text{mL}$ CMV IEp-LacZ, 106 $\mu\text{L}/\text{mL}$ SiMPs and 1.5% (vol/vol) Triton X-100 in HEPES; and (7) 106 $\mu\text{L}/\text{mL}$ CMV IEp-LacZ, 10.6 $\mu\text{g}/\mu\text{L}$ SiMPs, and 1.5% (vol/vol) Triton X-100 in HEPES. Suspensions were tapped to mix and allowed to incubate for 30 min at room temperature. Suspensions were centrifuged for 3 min at 10,000 rpm. 20 μL of supernatant was collected and loaded into wells of a 1% agarose gel. Gel electrophoresis was conducted at 200 V for 1 h. The gel was then photographed using a UV camera and volume was analyzed by standard image analysis software.

Surfactant-free transfection of cultured cells

HEK293 cells were seeded a density of 4×10^4 on glass cover slips in 12 35 mm dishes. Cultures were incubated for 48 h at 37°C with 5% CO_2 in air, in a humidified incubator. APTES-functionalized SiMPs were soaked in 1 mL 99.9% ethanol at room temperature in a sterile hood until ethanol evaporated completely. The present experiment was conducted in duplicate. SiMPs were then weighed out on a standard top-loading balance and suspended in DMEM complete medium at a concentration of 8 mg/mL. Total volume was divided equally into sterile Eppendorf tubes. 4 suspensions were prepared as follows: (1) 4.0 mg/mL SiMPs; (3) 0.89 ng/ μL CMV-IEp LacZ plasmid and 3.98 mg/mL SiMPs; (5) 2.8 mg/mL SiMPs and 29% Lyovec (vol/vol); and (6) 0.64 ng/ μL CMV-IEp LacZ plasmid, 2.9 mg/mL SiMPs, and 28% Lyovec (vol/vol). The following solutions were also prepared: (1) 0.89 ng/ μL CMV-IEp LacZ plasmid in DMEM medium and (2) 2.2 ng/ μL CMV-IEp LacZ plasmid in 99% (vol/vol) Lyovec. Lyovec is a commercially available lipophilic transfection reagent and functioned as a transfection control. 250 μL of each suspension/solution was tapped to mix and incubated for 30 min at room

temperature. 250 μL of each suspension/solution was added to the cover slips and cells were incubated for 30 min at room temperature in a sterile cell culture hood. Total volume of medium was brought to 1 mL. The final concentration of SiMPs, CMV-IEp LacZ plasmid, and Lyovec in all the corresponding wells is as follows, respectively: 1 mg/mL, 0.223 ng/ μL , 10% Lyovec (vol/vol). Cells were incubated for 48 h at 37°C with 5% CO_2 in air, in a humidified incubator. Following incubation, cells were assayed for LacZ expression according to the Dual-Luciferase Reporter Assay System protocol. Cells were visualized and counted using a Bright Line hemocytometer.

Surfactant-supplemented transfection of cultured cells

HEK293 cells were seeded a density of 2.0×10^4 on glass cover slips in 5 35 mm dishes. Cultures were incubated for 24 h at 37°C with 5% CO_2 in air, in a humidified incubator. APTES-functionalized SiMPs were soaked in 1 mL 99.9% ethanol at room temperature in a sterile hood until ethanol evaporated completely. SiMPs in cell culture medium [2 $\mu\text{g}/\mu\text{L}$] were ultra-sonicated via dispersion Protocol II. 5 solutions were prepared in cell culture medium in sterile Eppendorf tubes as follows: (1) cell culture medium only; (2) 6.0 $\mu\text{g}/\text{mL}$ CMV IEp-LacZ and 0.4 $\mu\text{g}/\mu\text{L}$ Lyovec; (3) 15 $\mu\text{g}/\text{mL}$ Triton X-100; (4) 6.0 $\mu\text{g}/\text{mL}$ CMV IEp-LacZ, 0.4 $\mu\text{g}/\mu\text{L}$ Lyovec, and 15 $\mu\text{g}/\text{mL}$ Triton X-100; (5) 0.3 $\mu\text{g}/\mu\text{L}$ SiMPs, 6.0 $\mu\text{g}/\text{mL}$ CMV IEp-LacZ, and 0.4 $\mu\text{g}/\mu\text{L}$ Lyovec. All solutions were tapped to mix and allowed to incubate at room temperature for 30 min in a sterile hood. 250 μL of each solution were added to each of the cover slips. Cells were incubated for 30 min at 37°C with 5% CO_2 in air, in a humidified incubator, after which the total volume of cell culture medium in the dishes was brought to 2 mL. Cells were incubated for 48 hr at 37°C with 5% CO_2 in air, in a humidified incubator. Following

incubation, cells were assayed for LacZ expression according to the Dual-Luciferase Reporter Assay System protocol. Cells were visualized and counted using a Bright Line hemocytometer.

RESULTS

Stain-etch preparation of silicon microparticles

While anodization of silicon wafers remains the most common preparative method for porous silicon formation, low cost and high throughput production makes stain-etching of metallurgical-grade silicon powder a practical alternative¹⁵. The etching process facilitates pore formation, expansion, and propagation within the microparticles, thereby increasing the surface area of the pSi. Subsequent surface oxidation provides ample sites for further functionalization and electrostatic coupling, as well as high bioavailability, that is the fraction of unchanged drug which reaches systemic circulation, as demonstrated by *in vitro* and *in vivo* studies of similar materials¹⁹.

Biocompatibility of silicon microparticles

The biocompatibility of micromaterials requires thorough investigation prior to *in vivo* application. Here we investigate the effects of both as-prepared and surface-oxidized SiMPs on viability and proliferation of HEK293 cells. Cells were treated with increasing concentrations [0.05, 0.5, and 5.0 mg/mL] of unconjugated SiMPs and assayed for cell viability at 24, 48, and 96 hours after treatment using the Trypan Blue exclusion assay. When treated with surface-oxidized SiMPs, we found no difference in cell viability when compared to the untreated control (**Fig 1**).

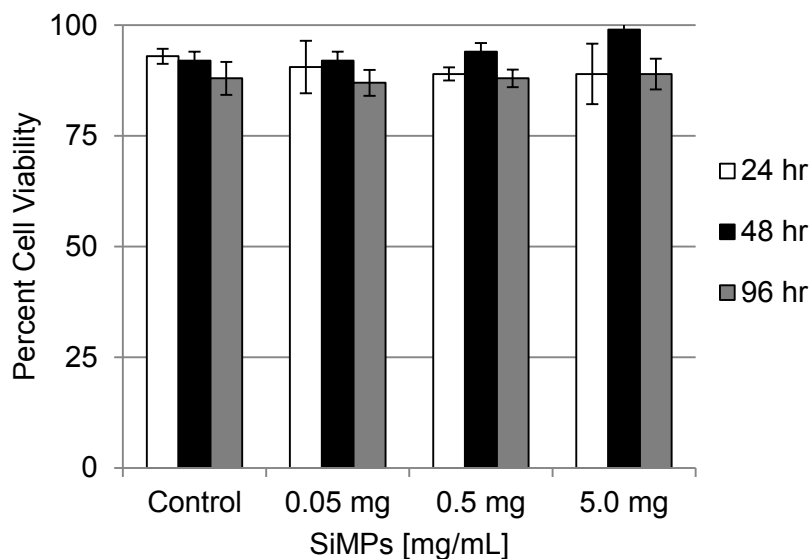


Figure 1 | Cytotoxicity of surface oxidized SiMPs on HEK293 cells as analyzed by Trypan blue exclusion assay. Cell-only control is included as reference (0 mg/mL). (*error bars represent standard deviations*)

Equivalent concentrations of as-prepared SiMPs were notably more cytotoxic than the surface-oxidized SiMPs at concentrations of 0.5 and 5 mg/mL (**Fig. 2**). Cellular proliferation following treatment with oxidized SiMPs was not affected when compared to the untreated control at concentrations at or below 0.5 mg/mL (**Fig. 3**). Similar effects were observed following treatment with as-prepared SiMPs.

Analysis of the *in vitro* cytotoxicity of both as-prepared and surface oxidized SiMPs suggest that surface oxidized material is more biocompatible with HEK293 cells. While as-prepared SiMPs failed to demonstrate toxicity at concentrations at and below 0.05 mg/mL, their oxidized counterparts were effectively non-toxic to HEK293 cells at concentrations up to 5 mg/mL. Thus the surface oxidized SiMPs were investigated further.

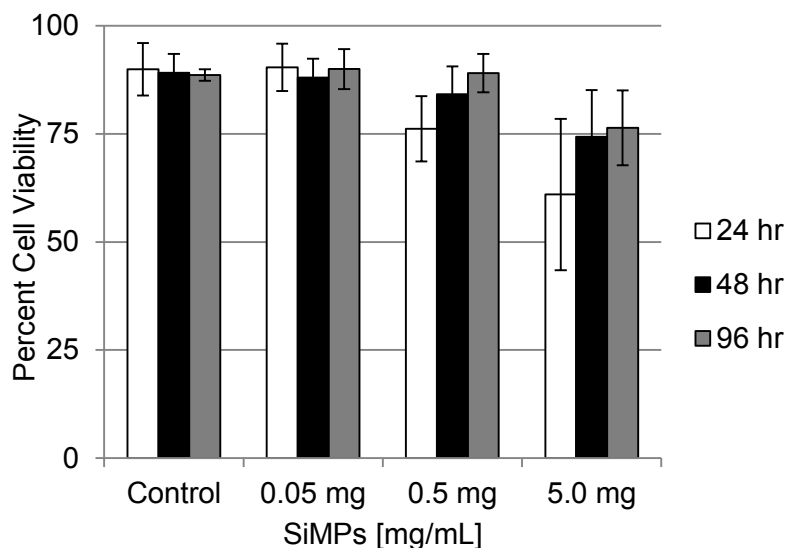


Figure 2 | Cytotoxicity of as-prepared SiMPs on HEK293 cells as analyzed by Trypan blue exclusion assay. Cell-only control is included as reference (0 mg/mL). (error bars represent standard deviations)

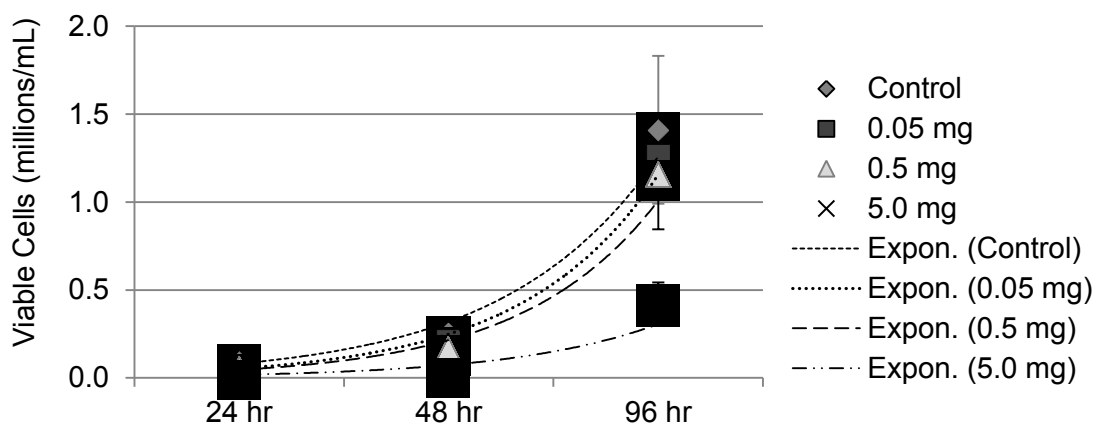


Figure 3 | Proliferation of HEK293 cells as analyzed by Trypan blue exclusion assay. Cells were incubated at 37°C with increasing concentrations of surface oxidized SiMPs [0, 0.05, 0.5, and 5.0 mg/mL] for 24, 48, and 96hrs. Cell-only control is included as reference (0 mg/mL). Exponential trend lines are shown for each condition. (error bars represent standard deviations)

Aminosilanization

Stain-etched, surface-oxidized MASE pSi microparticles (SiMP) are further modified using an aminosilanization route. (3-Aminopropyl)triethoxysilane (APTES) covalently links to the SiMPs at the oxidized surface. APTES protonates at biologically

neutral pH and thus provides a site for electrostatic coupling with negatively charged nucleic acids. Amino-functionalized cationic silica nanoparticles have been shown to electrostatically condense both genomic and plasmid DNA as well as prevent enzymatic degradation¹. Aminosilanization was shown to stabilize the nanoparticles in aqueous solution by decreasing their overall density and rigidity^{2,11}. In addition, silanisation routes have been used to facilitate protein adsorption and cellular adhesion onto inorganic surfaces¹¹. To determine the efficiency of APTES coupling, we fluorescently labeled APTES-functionalized SiMPs and visualized them using confocal microscopy.

FITC-coupling and imaging

The polydispersity and high porosity of the SiMPs can be exploited for efficient surface functionalization by either molecular tags or hybridization with nucleic acids. Here we visualize the size distribution of SiMPs via scanning electron microscopy (SEM) (**Fig. 4**). It is clear from these images that a relatively broad range of particle sizes is present in the sample.

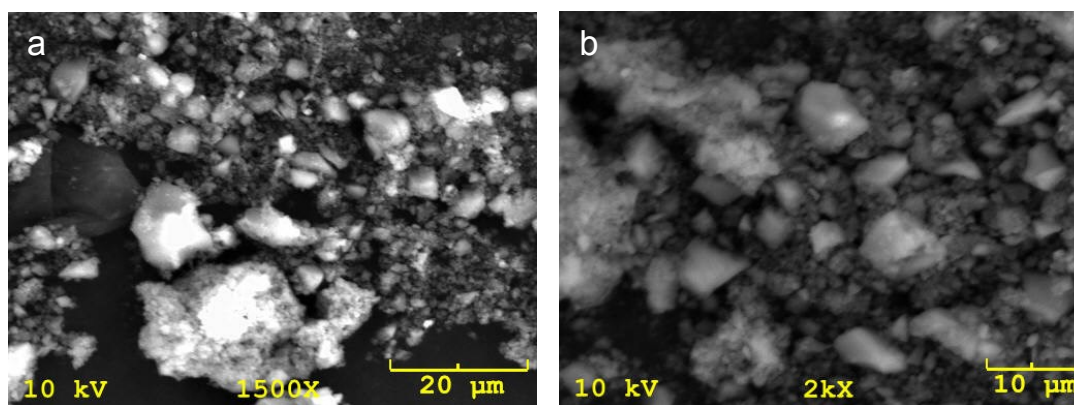


Figure 4 | SEM images of FITC-labeled APTES-functionalized SiMPs. (a) SiMPs demonstrate high polydispersity. (b) High magnification image

Some imaging and *in vitro* studies utilize fluorescent visualization of SiMPs. An efficient protocol for fluorescent labeling with a fluorescein derivative was developed. Fluorescein isothiocyanate (FITC) is a widely used fluorescent tag and can be easily visualized using traditional fluorescent and confocal microscopy. Sterilized SiMPs were conjugated with APTES followed by the fluorescein derivative FITC. The APTES covalently links to the oxidized surface and provides an amine function with which the FITC reacts. Efficient covalent linking between APTES and FITC has been used for labeling silica nanoparticles during droplet-based synthesis²⁰. Here we utilize the covalent linkage between APTES and FITC to determine the density of reactive primary amine groups on APTES-functionalized SiMPs, which are available for DNA binding. Two- and three-dimensional confocal microscopy reveals thorough fluorescent labeling. The uniform strong emission with FITC indicates a high density of reactive primary amine groups on the surface of the SiMPs as visualized by confocal microscopy (**Fig. 5**). An extended focus image shows yet again the high porosity and surface irregularity, as well as thorough fluorescent coupling (**Fig. 5b**). Here it is also possible to see extensive aggregation of SiMPs, as indicated by the size of the clusters (25-40 μm).

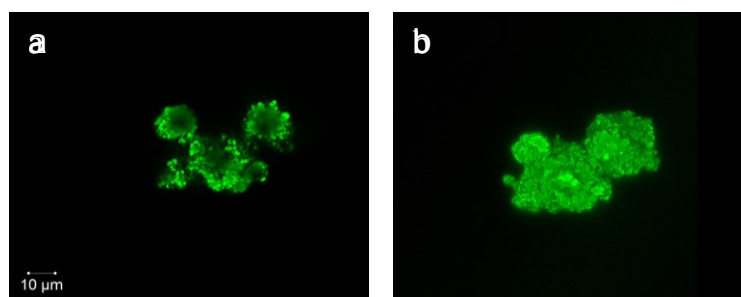


Figure 5 | FITC-conjugated SiMPs observed via confocal microscopy. **(a)** Two-dimensional image of a cluster of SiMPs. **(b)** Extended focus image of the same cluster represented in (a) was produced by a Z-stack program.

Dispersion

Due to their nonpolar silicon core, SiMPs are largely hydrophobic and insoluble in aqueous solution. Ultra-sonication has been shown to dramatically reduce the size distribution and toxicity of nano-scale particles, as well as increase their dispersion in aqueous solution²¹. Sonication prevented aggregation of 50 nm and 200 nm silica nanowires, which tend to clump together in solution¹⁶. Previous studies have shown that low frequency sonication does not affect covalently conjugated surface modifiers¹⁶. In order to minimize the aggregation and maximize the dispersion of APTES-functionalized SiMPs in cell culture medium, the material was subjected to one of two novel dispersion methods using ultra-sonication yielding the optimum concentration for *in vitro* studies. Protocol I was developed as a preliminary protocol to investigate the effect of low intensity ultra-sonication on particle structure and aggregation. Once no detrimental effects on particle structure were seen following Protocol I, a higher intensity protocol (Protocol II) was developed to further increase dispersion and decrease aggregation of SiMPs. The effectiveness of Protocol II at reducing SiMP aggregation was analyzed by TEM and shown to reduce the mean diameter of SiMPs (**Fig. 6**).

With a mean diameter of sonicated particles reduced to less than 430 nm using a novel dispersion method, we sought to determine if the SiMPs possess affinity for cultured cells. If so, the opportunity for entry into the cell is enhanced.

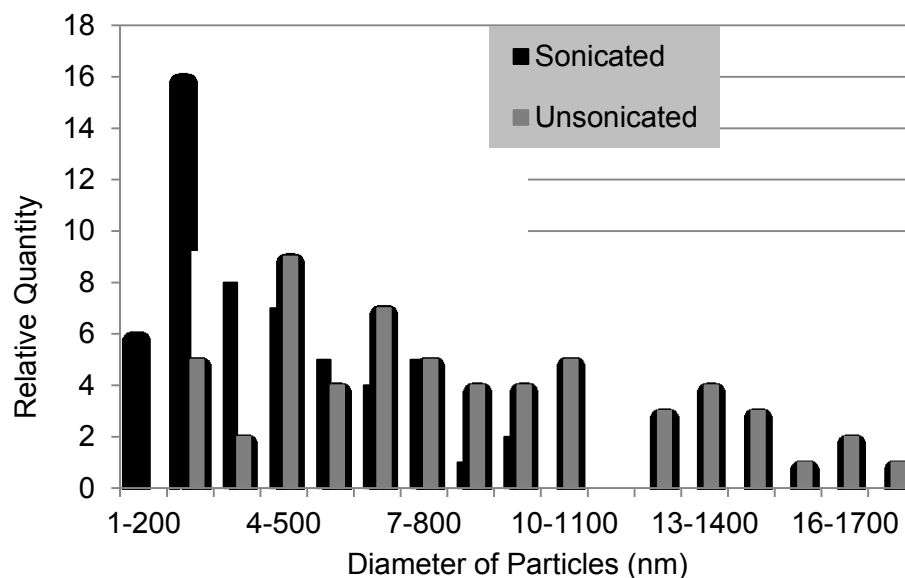


Fig. 6 | Size distribution of unsonicated and ultra-sonicated [3m, 4-5 W] APTES-MASE was analyzed by TEM. Diameter was taken from long axis of microparticles. Mean diameter of unsonicated microparticles [828.2 nm] was nearly double that of ultra-sonicated particles [421.9 nm].

Cellular interaction with fluorescently labeled silicon microparticles

Following dispersion via ultra-sonication (Protocol I), suspended microparticles isolated from the supernatant were then added to cells and allowed to incubate at 37°C for 48 hrs prior to visualization. FITC-conjugated SiMPs demonstrated high-affinity for HEK293 cells (**Fig 7**). Substantial aggregation along the cell membrane was observed (**Fig. 7**).

To better observe the interaction between SiMPs and the cell membrane, immunocytochemistry was used to fluorescently label beta-actin, a component of the cytoskeleton of the cell. Thorough coating of cell with SiMPs demonstrates the high affinity interaction between the cell membrane and the SiMPs (**Fig. 8**). This phenomenon is most likely due to the electrostatic attraction between the positively charged amino function on uncoupled APTES and the negative charge of the outer leaflet of the cell membrane.

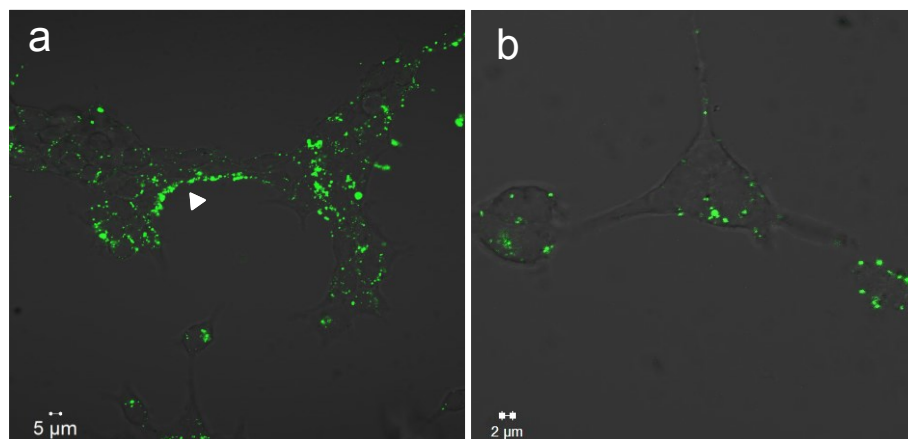


Figure 7 | FITC-conjugated SiMPs demonstrate high-affinity for HEK293 cells as visualized by overlays of confocal and differential interference contrast images. **(a)** Arrows indicate areas where microparticles coat the cell membrane. **(b)** Highly dispersed SiMPs interact with three individual cells.

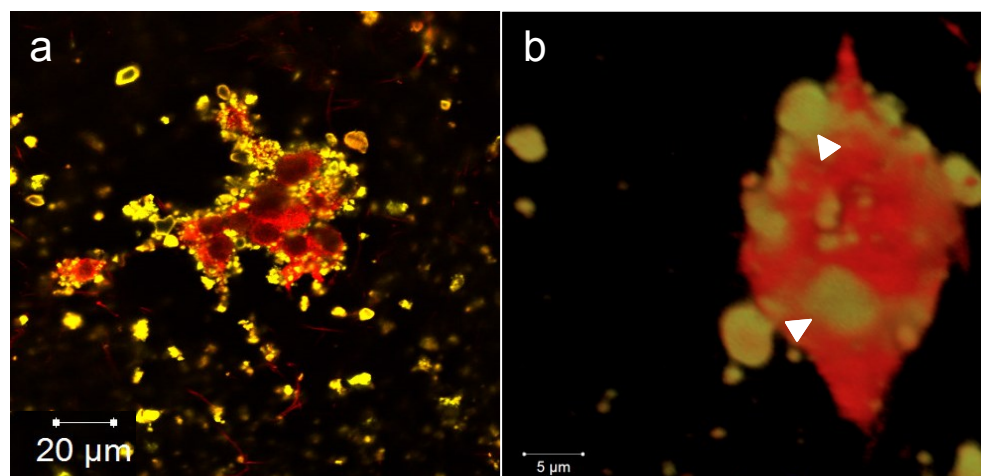


Figure 8 | **(a)** Two dimensional image of actin immunofluorescence stained HEK293 cells (red) with FITC-conjugated MASE pSi microparticles (yellow) **(b)** Extended focus image via Z-stack shows adsorption of FITC-labeled microparticles onto the membrane of an actin-labeled HEK293 cell. *(Arrows indicate regions where absorption can be clearly observed)*

Imaging of immunofluorescently-stained 293HEK cells treated with FITC-labeled SiMPs is shown to be an effective method to study the nature of the interaction

between cultured human cells and SiMPs. A three-dimensional rendering of this interaction shows overlapping fluorescence of the SiMPs and the cell membrane, suggesting that the SiMPs adsorb to the cell membrane and/or integrate into the membrane. We are unable to determine using this method of microscopy whether SiMPs are able to enter the cytosol of the cell.

DNA binding

The ability to sequester nucleic acid is paramount for successful and efficiency gene delivery. A protonated amine function on the surface of silica nanoparticles is able to electrostatically couple to plasmid DNA¹. Here we employ the protonated amine group on the end of APTES functionalized to the surface of SiMPs to sequester plasmid DNA in a biological buffer, HEPES. HEPES was used as a solvent in order to imitate biological conditions, such as pH. Following dispersion via Protocol II, APTES-functionalized SiMPs are shown to possess electrostatic DNA-binding capability that is dependent on silicon:DNA mass ratios at ratios higher than 1:1 Si:DNA (**Fig. 9**).

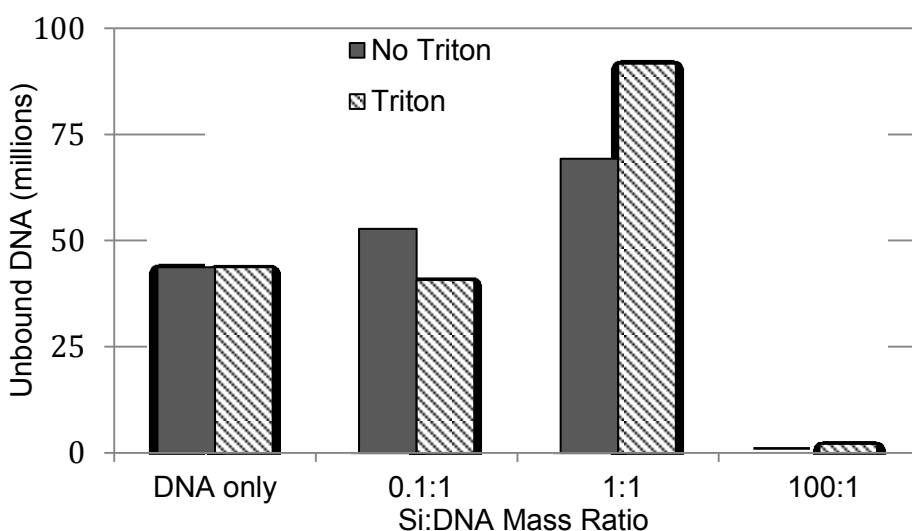


Fig. 9 | APTES-MASE pSi microparticles were electrostatically coupled to the CMV-LacZ plasmid at varying silica:DNA mass ratios. Triton X-100 was added to indicated samples. DNA-binding efficiency was analyzed via gel electrophoresis.

Surfactants are compounds that lower the surface tension between two liquids or a liquid and a solid. Surfactants are commonly used to permeabilize or disrupt the cell membrane of cultured cells; however more recently surfactants have been investigated for their potential in aiding with cellular uptake of nanomaterials²². Polymeric nanoparticles coated in a non-ionic surfactant have been shown to deliver the drug doxorubicin across the blood brain barrier of rats at therapeutically useful concentrations²³. It is thought that the lipophilicity of non-ionic surfactants enables them to bind certain lipoprotein receptors on the cell surface and well as integrate into the membrane²³. In the present study, we sought to determine if the non-ionic surfactant Triton X-100 (polyethylene glycol p-(1,1,3,3-tetramethylbutyl)-phenyl ether) had an effect on the DNA binding capabilities of APTES-functionalized SiMPs. The surfactant was added to the suspension of SiMPs and plasmid DNA in HEPES. After analysis of unbound DNA by gel electrophoresis, we found no conclusive effect on DNA binding by Triton X-100.

Transfection with plasmid DNA

A practical and successful transfection vector must exhibit minimal toxicity in a biological system, a strong affinity for target cells, and the ability to facilitate the delivery of the gene or drug across the cell membrane. Using these parameters, we investigated SiMPs as a practical transfection vector in an *in vitro* environment. We have shown that SiMPs are biocompatible with cultured human cells, interact strongly with the cell membrane, and can sequester DNA. Previously reported studies have demonstrated that nanoparticles of various compositions are able to facilitate transfection in cultured cells¹. By a mechanism not yet fully understood, APTES-coupled silica nanoparticles ($\approx 30\text{nm}$)

have shown to successfully deliver and induce expression of the pEGFP vector into COS-1 cells¹. In addition, similarly sized nanoparticles demonstrate the capacity to deliver water-insoluble photosensitizing drugs used in anti-cancer therapy to the cytoplasm of tumor cells *in vitro*²⁴. In the present work, the ability of polydispersed APTES-functionalized SiMPs to deliver plasmid DNA to 293HEK cells and induce expression of a reporter gene was investigated.

Unsonicated APTES-functionalized SiMPs were analyzed first for gene delivery ability. Following incubation with the CMV-IEp LacZ plasmid encoding the reporter gene for β -galactosidase, suspensions were added to 293HEK cells. The cells were then assayed for β -galactosidase expression, as demonstrated by the production of the blue product resulting from the cleavage of X-gal. Here we do not observe β -galactosidase expression in cells treated with a suspension of SiMPs and the reporter plasmid (**Fig. 10**).

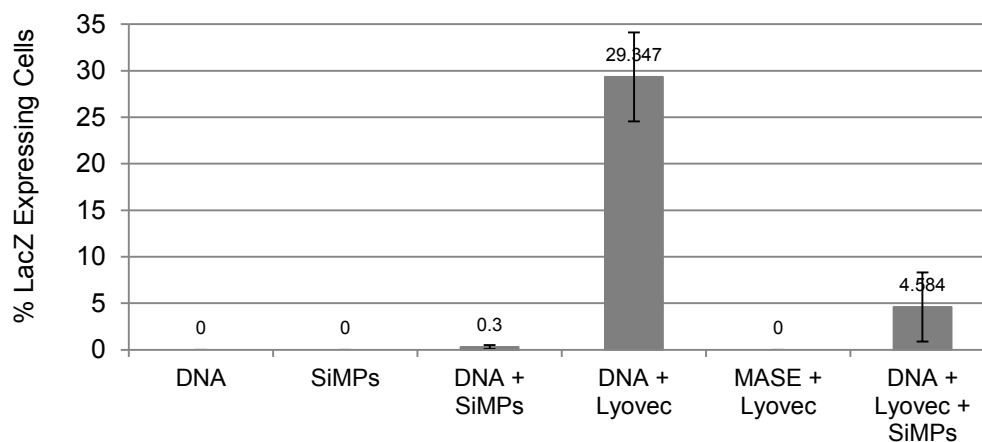


Fig. 10 | Transfection efficiency of 293HEK cells treated with APTES-functionalized SiMPs or APTES-functionalized SiMPs and Lyovec, a commercially available lipophilic transfection vector. (*error bars represent standard deviations*)

To determine the effect of a reduced particle size on the gene delivery capabilities of ultra-sonicated APTES-functionalized SiMPs, SiMPs were ultra-sonicated via Protocol

II and a similar protocol was conducted to assay for CMV-IEp LacZ expression in 293HEK cells, in the absence and presence of the surfactant Triton X-100. However after visualization by light microscopy, the cells treated with Triton X-100 exhibited morphological characteristics of cell death. We concluded that the concentration of Triton X-100 used was cytotoxic to 293HEK cells.

DISCUSSION

Thermally-oxidized mesoporous silicon microparticles represent a practical alternative to traditional delivery methods due to their biocompatibility, surface reactivity, high surface area-to-volume ratio, and aqueous degradation properties. Metal-assisted stain etching as a porosification method is an appealing alternative to anodization because of simplicity and relatively lower cost of production. Although the literature may suggest that the most promising inorganic gene delivery vectors are less than 100nm in size, it should be noted that, although the particles investigated here fall have a micro-scale diameter distribution ($D_{10}=0.7\mu\text{m}$, $D_{50}=2.2\mu\text{m}$, $D_{90}=8.9\mu\text{m}$), our SiMPs possess nano-scale properties such as nano-scale pores and high surface area.

We show here that SiMPs are non-toxic and have minimal effect on cell proliferation of HEK293 cells. Furthermore, we demonstrate the ability of FITC-labeled SiMPs to adsorb onto the membrane of HEK293 cells with high-affinity. Immunofluorescent staining of cellular cytoskeletal components reveals no visible effect on cell morphology following treatment with SiMPs. Since ideal gene delivery vectors should possess tunable biodegradability, we demonstrate the ability to reduce the size distribution of SiMPs via a novel ultra-sonication method. An inverse correlation between thickness of silicon and biodegradability has been shown in silicon nanotubes¹⁴.

In the present study, we also show the ability of APTES-functionalized SiMPs to electrostatically bind plasmid DNA at physiological pH. Further investigation is needed to confirm these results and determine the ideal Si:DNA mass ratio which yields optimum binding. Although SiMPs were not shown to facilitate transfection in 293HEK cells, these findings highlight the feasibility of employing SiMPs for gene delivery. We intend to further investigate what is required to increase the transfection efficiency of SiMPs.

REFERENCES

1. I. Roy, T. Y. Ohulchansky, R. A. Mistretta, D. J. Bharali, N. Kaur, H. Pudavar, and P. N. Prasad, Optical tracking of organically modified silica nanoparticles as DNA carriers: A nonviral, nanomedicine approach for gene delivery, *Proc Natl Acad Sci U. S. A.*, 2005, **102**, 279–284.
2. D. J. Bharali, I. Klejbor, E. K. Stachowiak, P. Dutta, I. Roy, N. Kaur, E. J. Bergey, P. N. Prasad, and M. K. Stachowiak, Organically modified silica nanoparticles: A nonviral vector for in vivo gene delivery and expression in the brain, *Proc Natl Acad Sci U. S. A.*, 2005, **102**, 11539-11544.
3. S. Fumoto, S. Kawakami, M. Hashida, and K. Nishida. *Novel Gene Therapy Approaches*, Ed. Ming Wei and David Good, Rijeka, Croatia: InTech, 2013.
4. A. Surendiran, S. Sandhiya, S. C. Pradham, and C. Adithan, Novel applications of nanotechnology in medicine, *Indian J Med Res*, 2009, **130** (6), 689-701.
5. L. Gu, Biodegradable porous silicon nanomaterials for imaging and treatment of cancer, *Electronic Theses and Dissertations at University of California San Diego*, 2012, 1-173.
6. R. K. Jhal, P. K. Jhal, K. Chaudhury, S. V. S. Rana, and S. K. Guha, An emerging interface between life science and nanotechnology: present status and prospects of reproductive healthcare aided by nano-biotechnology, *Nano Reviews*, 2014, **5**, 22762-22780.
7. A. Vaseashta, and D. Dimova-Malinovska, Nanostructured and nanoscale devices, sensors, and detectors, *Sci Technol Adv Mat*, 2005, **6** (3-4), 312-318.
8. A. Z. Wilczewska, K. Niemirowicz, K. H. Markiewicz, and H. Car, Nanoparticles as drug delivery systems, *Pharmacol Rep*, 2012, **64**, 1020-1037.
9. F. Alexis, E. Pridgen, L. K. Molnar, and O. C. Farokhzad, Factors Affecting the Clearance and Biodistribution of Polymeric Nanoparticles, *Mol Pharm*, 2008, **5** (4) 505-515.
10. E. J. Anglin, L. Cheng, W. R. Freeman, and M. J. Sailor, Porous silicon in drug delivery devices and materials, *Adv Drug Deliver Rev*, 2008, **60** (11), 1266–1277.
11. S. P. Low, K. A. Williams, L. T. Canham, and N. H. Voelcker, Evaluation of mammalian cell adhesion on surface-modified porous silicon, *Biomaterials*, 2006, **27** (26), 4538–4546.

12. D. Fan, G. R. Akkaraju, E. F. Couch, L. T. Canham, and J. C. Coffey, The role of nanostructured mesoporous silicon in discriminating in vitro calcification for electrospun composite tissue engineering scaffolds, *Nanoscale*, 2010, **3**, 354-361.
13. S. Su, L. Lin, Z. Li, J. Feng, and Z. Zhang, The fabrication of large-scale sub-10-nm core-shell silicon nanowire arrays, *Nanoscale Res Lett*, 2013, **8** (405), 1-7.
14. X. Huang, R. Gonzalez-Rodriguez, R. Rich, Z. Gryczynski, and J. Coffey, Fabrication and size dependent properties of porous silicon nanotube arrays, *J L Chem Commun*, 2013, **49**, 5760-5762.
15. A. Loni, D. Barwick, L. Batchelor, J. Tunbridge, Y. Han, Z. Y. Li, and L. T. Canham, Extremely High Surface Area Metallurgical-Grade Porous Silicon Powder Prepared by Metal-Assisted Etching, *Electrochem Solid St*, 2011, **14** (5) K25-K27.
16. S. M. Nelson, T. Mahmoud, M. Beaux 2nd, P. Shapiro, D. N. McIlroy, and D. L. Stenkamp, Toxic and teratogenic silica nanowires in developing vertebrate embryos, *Nanomedicine*, 2010, **6** (1), 93-102.
17. H. Huiyuan, A. Nieto, F. Ma, W. R. Freeman, M. J. Sailor, and L. Cheng, Tunable sustained intravitreal drug delivery system for daunorubicin using oxidized porous silicon, *J Control Release*, 178, 46-54.
18. Q. Chen, Y. Xue, and J. Sun, Kupffer cell-mediate hepatic injury induced by silica nanoparticles in vitro and in vivo, *Int J Nanomedicine*, 2013, **8**, 1129-1140.
19. S. P. Low, N. H. Voelcker, L. T. Canham, and K. A. Williams, The biocompatibility of porous silicon in tissues of the eye, *Biomaterials*, 2009, **30** (15), 2873-2880.
20. J. B. Wacker, I. Lignos, V. K. Parashara, and M. A. M. Gijssels, Controlled synthesis of fluorescent **silica** nanoparticles inside microfluidic droplets, *Lab Chip*, 2012, **12**, 3111-3116.
21. M. Kang, C. Lim, and J. Han, Comparison of Toxicity and Deposition of Nano-Sized Carbon Black Aerosol Prepared With or Without Dispersing Sonication, *Toxicol Res*, 2013, **29** (2), 121-7.
22. S. P. Samuel, N. Jain, F. O'Dowd, T. Paul, D. Kashanin, V. A. Gerard, Y. K. Gun'ko, A. Prina-Mello, Y. Volkov, and S. P. Samuel, Multifactorial determinants that govern nanoparticle uptake by human endothelial cells under flow, *Int J Nanomedicine*, 2012, **7**, 2943-2956.
23. S. Wohlfart, A. S. Khalansky, S. Gelperina, O. Maksimenko, C. Bernreuther, M. Glatzel, and J. Kreuter, Efficient Chemotherapy of Rat Glioblastoma Using Doxorubicin-Loaded PLGA Nanoparticles with Different Stabilizers, *PLoS ONE*, 2011, **6** (5), e19121.

24. I. Roy, T. Y. Ohulchanskyy, H. E. Pudavar, E. J. Bergey, A. R. Oseroff, J. Morgan, T. J. Dougherty, and P. N. Prasad, Ceramic-Based Nanoparticles Entrapping Water-Insoluble Photosensitizing Anticancer Drugs: A Novel Drug-Carrier System for Photodynamic Therapy, *J Am Chem Soc*, 2003, **125** (26), 7860–7865.